JOURNAL OF OPTOELECTRONICS AND ADVANCED MATERIALS, Vol. 10, No. 12, December 2008, p. 3317 - 3321

Studies on static and dynamic light scattering properties of water based magnetic fluid

D. CHICEA*, M. RĂCUCIU
"Lucian Blaga" University, Faculty of Science, Dr. I. Ratiu Street, No.5-7, 550024, Sibiu, Romania,

Magnetic fluids (ferrofluids) are dispersions of small, single-domain magnetic particles suspended in a fluid carrier. In this work magnetite nanoparticles coated with different surfactants (tetramethylammonium hydroxide, perchloric acid and citric acid) and dispersed in water were used as light scattering targets. The water based magnetic fluid samples were prepared by a co-precipitation method. A simple experimental setup was assembled to analyze the magnetic fluid static and dynamic light scattering properties. The setup consists of a He-Ne laser, a cuvette, a sensitive detector, a data acquisition system and a computer. Light scattering intensity at small angles was measured and the anisotropy parameter g was determined by the mean square method using a code that was written for this purpose. The variation of the light scattering anisotropy parameter **g** with the nanoparticles type is discussed. The far interference field presented the typical "boiling speckles" aspect caused by the complex motion of the scattering centers. The average intensity and contrast were calculated for each movie in order to compensate the fluctuations. The variation of these parameters with the magnetic fluid concentration was found and plotted. Time series were recorded for different nanoparticles types, the autocorrelation time was calculated for each sample and the variation of the autocorrelation time with the particle type is discussed.

(Received September 27, 2008; accepted November 27, 2008)

Keywords: Ferrofluids, Light scattering, Nanoparticles

1. Introduction

The ferrofluids (magnetic fluids) represent a well defined category of magnetically controllable nanomaterials with fluid properties. Ferrofluids or magnetic fluids are stable colloidal homogeneous suspensions of small, single-domain magnetic particles (around 10nm in diameter) in an aqueous or non-aqueous carrier fluid [1-2]. Iron oxide (usually magnetite (Fe_3O_4) and maghemite (Fe_2O_3)) nanoparticles are the most frequently used magnetic particles in ferrofluids, due to their high saturation magnetization and high magnetic susceptibility [3]. Due to the small size of the magnetic particles and to the superparamagnetic behavior, ferrofluids have been extensively used in several technological and biomedical applications [4–5].

Dynamic and static light scattering experiments became important tools for the investigation and characterization of structural properties of complex fluids, e.g. colloids [6-9]. In theoretical studies of light scattering on ferrofluids, extensive particle association into chainlike and ringlike clusters was observed at low concentration [10].

The ferrofluids are opaque to visible light, therefore the ferrofluid particles concentration must be very small for light scattering experiments.

When coherent light crosses a suspension, a speckled image, having a statistical distribution of the intensity over the interference field is obtained. The speckled image appears as a result of the interference of the wavelets scattered by the scattering centers, each wavelet having a different phase and amplitude in each location of the interference field. The scattering centers (SC hereafter) complex movement produces fluctuations of the image intensity in each location of the interference field. These fluctuations give the aspect of "boiling speckles" [11], [12].

The speckled image can be observed either in free space and is named objective speckle or on the image plane of a diffuse object illuminated by a coherent source; it is named subjective speckle in [11]. The review paper [12] nominates the two types of speckled images far field speckle and image speckle. In this work the objective speckle, respectively far field speckle is considered.

The Speckle dynamics analysis has become a current method to characterize the dynamic behavior of scattering medium such as flow, sediment and Brownian movement. The motion of the speckle field was analyzed by correlometric methods [13-15] or by laser speckle contrast analysis [15-17]. The speckle size can be used to measure the roughness of a surfaces [18-20] or to determinate the thickness of semi-transparent thin slab like in [21]. Most of the above mentioned experiments use the backscattered light speckle configuration. In papers like [22] a different optical set-up is used to measure the correlation function in the near field, and show the near-field speckle dependence on the particles size. The work reported in [23-24] uses a transmission optical set-up to measure the far field parameters like contrast and speckle size. The transmission type of setup was used in the work.

The next sections present briefly the ferrofluid synthesis and in detail the optical experimental setup and the results of the far field interference pattern analysis.

2. Experimental

2.1 Ferrofluid synthesis

Magnetite nanoparticles were prepared by alkaline hydrolysis (in the aqueous ammonia solution presence) of the concentrated mixed solution of the ferric and ferrous salts solutions in presence of 2M HCl solution following the steps presented in [25]. The magnetite suspensions were finally washed with deionized water to reach approximately 6.5 pH value. After washing, the magnetic particles aggregation was prevented by using 25% solution of tetramethylammonium hydroxide as surfactant for S1, perchloric acid for S2 and citric acid for S3, under continuous (sixty minutes) and vigorous mechanically stirring. The water based magnetic fluid samples synthesized in our laboratory kept their colloidal characteristics for up to 6 months and low level of magnetic fluid nanoparticles sedimentation in time was observed.

For measuring the physical magnetic nanoparticles diameters we used a TESLA transmission electron microscop. The TEM images were produced by a device with a resolution of 1.0nm. For the three magnetic fluid samples that were analysed, the TEM micrographs showed that the magnetic nanoparticle size ranges between 6 nm and 21 nm, exhibiting mostly spherical shape.

The volume fraction Φ of ferromagnetic phase particles in the ferrofluid samples was determined from mass density measurements according to the equation:

$$\Phi = \frac{\rho_F - \rho_L}{\rho_S - \rho_L} \tag{1}$$

where ρ_F is the density of the ferrofluid, ρ_L the density of the carrier fluid, and ρ_S the density of the solid particles. Density was measured by means of picnometric method at T = 295K and the results are presented in Table I together with the dimensional analysis results.

Table 1. The dimensional analysis data and volume fraction of the ferrofluids samples

Ferrofluid sample	Surfactant molecule	Φ (%)	d_{TEM} (nm)
S1	tetramethylammonium hydroxide	2	7.2
S2	perchlorate	4.5	10.5
S3	citrate	5	11.4

2.2 Light scattering experimental setup

A transmission type of experiment was set-up. The schematic is presented in Fig. 1. The He-Ne laser had a wavelength of 632 nm and a constant power of 2 mW. The active area of the glass cuvette was 12 mm thick. Measurements were done at 3.5 degrees from the beam axis using a CMOS camera and data acquisition was done on a PC using the USB port and the far field speckle was recorded, not the speckle image.

For light scattering anisotropy studies, the initial ferrofluids samples (presented in Table I) were diluted at a volume ratio of $3.0*10^{-6}$. Such a small volume ratio was used because the cuvette was a standard cuvette, not a specially thin one and the optical depth of the sample was maintained around 1, in order to prevent multiple scattering, which modifies the value of the anisotropy parameter *g*. The dilution of the water based magnetic fluid samples was done using deionized water right before the light scattering analysis, by slowly adding the necessary amount of deionized water and vigurously stirring (using a mechanic stirrer for few minutes), in order to reduce the magnetic particles agglomeration rate that actually begins during dilution. The light scattering experiments, performed in two different ways, as described in the next section, lasted for a short time. The first type of experiments, conducted for measuring the average intensity and contrast, lasted for 60 seconds for each sample (dilution).

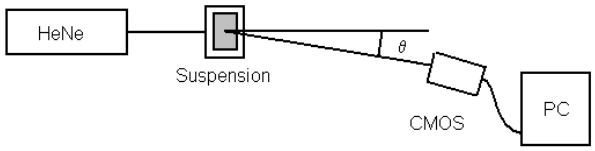

Fig. 1 The schematic of the experiment, seen from above.

In order to analyze the dynamic light scattering properties and the light scattering anisotropy the CMOS camera was replaced by a detector, which was a phototransistor. The light scattering intensity was measured at different small angles. Each measurement lasted for 120 seconds per angle and the light intensity at was measured at 10 angles; therefore the time span of the experiment was 20 minutes.

2.3 Data processing

The average contrast of the image, either acquired as a bitmap or extracted from the frames of the movie, is calculated [11], [23], and [24] as:

$$C = \frac{\sqrt{< \left(I(i,j) - < I > \right)^2 >}}{< I >} \tag{2}$$

where $I(i,j)=I(x_i, y_j)$ is the intensity recorded by the cell (i,j) of the CMOS, hence by the pixel (i,j) of the array of pixels the image consists of. This is a space contrast and not a time contrast, as described in [26]. In (2) the angular brackets stand for average over the entire 640x480 collection of intensity values for the image that is processes.

The average scattered light intensity was calculated by averaging the values recorded in each one of the 640x480 pixels the image consists of. The color depth was 24 bits.

In the first part of the experiment a bitmap image,

having a resolution of 640x480 pixels was recorded for different dilutions. Using a program written for this purpose the average intensity over the recorded area and the average contrast were calculated. Examining the results we notice a big spread of the data in a small concentration range, caused by the fluctuations. In order to compensate the fluctuations, an uncompressed, 24 bits AVI type movie was recorded for each concentration, using a framerate of 1 per second and the same resolution, 640x480 pixels. The average over the 120 frames for each sample did not depend on the specific time they were recorded at and the results presented further on, regarding the contrast and intensity are the averages as described above.

Another type of measurements we did using a modified version of the experimental setup in Fig. 1 were connected to the light scattering anisotropy. The CMOS camera was replaced by a photodetector having an angular opening of 0.002 radians or 0.1273 degrees. We used the typical light scattering procedure, with collimated laser beams, detecting the far field [27], in assessing the light scattering properties of the nanoparticles from the magnetic fluid. The single scattering act can be described by the one parameter Henyey Greenstein phase function (1) [26].

$$f(\mu)=\frac{1}{2}\frac{1-g^2}{\left(1-2\mu g+g^2\right)^{\frac{3}{2}}} \tag{3}$$

with $\mu=\cos(\theta)$.

The light intensity that can be measured using a detector is proportional with the integral F of the phase function over the polar angle interval $[\theta_1, \theta_2]$ covered by detector. The function, F in (4) was fit on the experimental data acquired at different small angles with a program written for this purpose, using the least squares method. The results are presented in the next section.

$$F(\mu_1,\mu_2)=\int_{\mu_1}^{\mu_2} f(\mu)d\mu=\frac{I_0(1-g^2)}{g}\left[\frac{1}{\sqrt{1+g^2-2g\mu_1}}-\frac{1}{\sqrt{1+g^2-2g\mu_2}}\right] \tag{4}$$

The constant I_0 in (5) is proportional both with the SC concentration and with the light scattering cross section of one individual SC.

The light scattering dynamics was analyzed as well. Using the same detection setup as previously described, a time series was recorded for each sample for 360 seconds with the detector placed at $\theta=0^o$ 30'.

The autocorrelation function for each sample was calculated as [24]:

$$A(\tau)=\frac{\langle I(\vec{r},t)*I(\vec{r},t+\tau)\rangle}{\langle I(\vec{r},t)*I(\vec{r},t)\rangle} \tag{5}$$

where the angle brackets denote averages over time t, r represents the position of the CMOS conversion matrix, and τ is the correlation time. The normalized autocorrelation function decreases from 1 and we can define the autocorrelation time τ_c as the time when the autocorrelation function decreases to 1/e. The autocorrelation time for the samples was calculated using the procedure described above and the results are presented in the next section.

3. Results

The static properties of the far interference field, like average intensity, speckle size and contrast were measured for three samples, S1, S2 and S3, over a big concentration range. Figure 2 presents the variation of the average contrast with the concentration for sample S1. The error bars on the plots are the confidence intervals calculated with the Student test, for 120 samples (frames) for each sample and a 99% confidence level, using:

$$l=\frac{t\cdot S}{\sqrt{n}} \tag{6}$$

where t is the parameter of the Student test, S is the dispersion and n is the number of frames, 120 for this experiment. More details on the algorithm, procedure and on the programs used in calculating the static parameters are presented in [29] and [30] and the variation of the average intensity and average speckle size with the concentration are presented in [31].

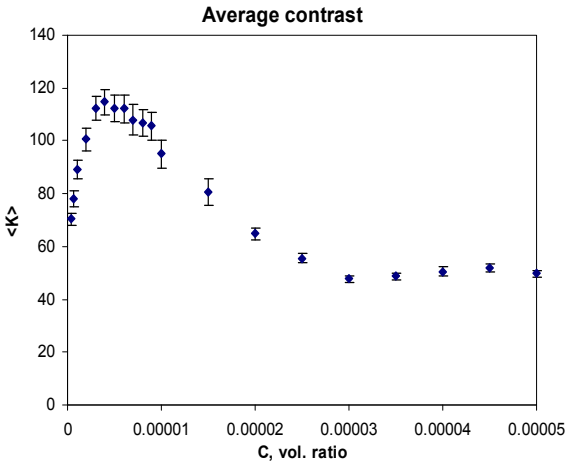

Fig. 2 The average contrast variation with the concentration for S1.

Examining the experimental results, presented in [31] and in Fig. 2 for S1 and not presented here for S2 and S3 we notice that at very small ferrofluid concentration the average intensity increases with the nanoparticles concentration, presents a maximum around 10^{-5} and then decreases with the concentration. As the concentration increases in the range where multiple scattering is dominant, the average intensity remains constant.

The average contrast, presented in Fig. 2, has a very

fast increase with the SC concentration, a maximum followed by a fast decrease. When the concentration increases the slope decreases in module and finally the concentration remains constant. This variation is similar with the work reported in [23], where organic SCs were used.

The light scattering anisotropy was measured for the three types of samples using the experimental setup and the procedure described in the previous section. The results of the fit are presented in Table II.

Fig. 3 presents the plot of the experimental data and of the F function calculated with the I_0 and g values from the fit for sample S2. Examining Table 2 we notice that the anisotropy parameter g decreases with the increase of the particle diameter, which means that the smaller the nanoparticle size is, the more forward peaked the scattered light intensity is.

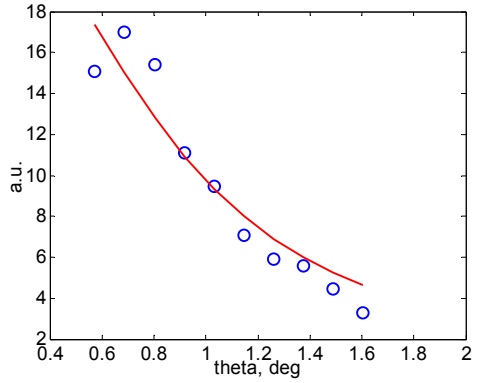

Fig. 3 The plot of the experimental data (circles) and of the calculated F function (solid line) for sample S2.

Table 2. The results of the light scattering anisotropy measurement on the three magnetic nanofluid samples

No	Sample	I_0, a.u.	ΔI_0, a.u.	g	Δg
1	S1	201.3	0.02	0.99533	$5*10^{-5}$
2	S2	233.6	0.03	0.99108	10^{-5}
3	S3	304.2	0.01	0.98219	$5*10^{-6}$

Moving to the I_0 constant, as the volume ratio of the nanoparticles was the same, that is $3.0*10^{-6}$, we notice an increase of the I_0 value with the particle size, which is in good agreement with the theory. As the particle diameter *d* increases, at constant volume ratio the nanoparticles *N* number should vary with the diameter *d* as:

$$N = \frac{V}{\frac{4\pi}{3}\cdot\left(\frac{d}{2}\right)^3} \quad (7)$$

In (7) *V* is the toal nanoparticles volume. Light scattering on nanoparticles is a Rayleigh type of scattering, therefore the light intensity scattered by one individual particle is proportional to d^6 [32]. The average intensity scattered by all the nanoparticles in the sample and recorded at a constant angle is therefore proportional to d^3, thus increasing with the nanoparticles diameter.

Moving to the anisotropy parameter g, we find a surprising result. As the light scattering is a Rayleigh type scattering, the anisotropy should be described by the factor $(1+\cos^2\theta)$ [32], totally independent of the nanoparticle diameter, while the Henyey Greenstein phase function (1) describes Mie scattering, typical for particles having a diameter comparable with the wavelength, which for this experiment was 632 nm. The very big values that were found in this experiment are typical for bigger particles, having a diameter bigger than the wavelength. This result, suggests that in a matter of minutes the magnetic nanoparticles agglomerates were formed in suspensions, scattering light as a whole not as individual scatterers. This result are similar with the light scattering experiments reported in [33] on magnetite particles dispersed in kerosene, where agglomeration was induced by magnetic field. In [33] the increasing of the light scattered at 23^o was an indication of increasing the agglomerates size while in this work the increase of the anisotropy parameter *g* at values close to 1 indicates the existence of clusters having a diameter comparable with 0.632 μm.

The third type of experiment, on light scattering dynamics analysis done on the time series recorded using the procedure described in the previous section was done on 180 seconds records. Fig. 4 presents the autocorrelation function for the time series recorded for sample S1.

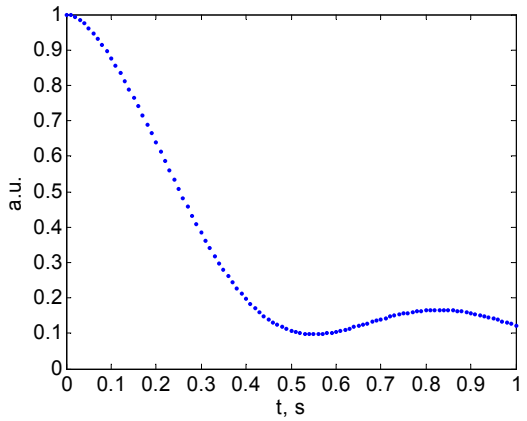

Fig. 4 The plot of the autocorrelation function for sample S1. The autocorrelation time is 0.30 seconds.

The values of the autocorrelation time for the three samples are presented in Table III.

Table 3. The autocorrelation time for the three samples

No.	Sample	Autocorrelation time, s
1	S1	0.30
2	S2	1.17
3	S3	1.29

We notice that the autocorrelation time increases with the magnetic nanoparticle size, if the samples have the same volume ratio. This result is consistent with the typical procedure for particle sizing by light scattering [34], which has already been used for some time in commercial applications like [35], where the hydrodynamic diameter is measured, rather than the physical diameter in electron microscopy or the optical diameter, using light scattering anisotropy experiments.

4. Conclusions

This paper presents the results of our investigation on the light scattering properties of diluted ferrofluid nanoparticles. They reveal that the average speckle contrast and light intensity have a fast increase with the SC increase in the very small concentration, that is $0 – 10^{-5}$ volume ratio followed by a slow decrease in the range 10^{-5}-10^{-4} volume ratio. This trend of the curves can be used in measuring the ferrofluid nanoparticles concentration, in the extremely small concentration range, that is $0 – 10^{-5}$. We also found that the autocorrelation time increases with the increase of the magnetic nanoparticles size.

Moreover, the light scattering anisotropy parameter g we measured presents elevated values, very close to 1, indicating that at very small concentrations the agglomeration process is so fast, that in a matter of a few minutes a considerable part of the nanoparticles can be found in agglomerates, scattering coherent light as a 0.1 – 1 micron sized object, rather than individual.

References

[1] R.E. Rosensweig, Ferrohydrodynamics, Cambridge University Press, Cambridge (1985).
[2] S. Odenbach (Ed.), Ferrofluids: Magnetically Controllable Fluids and Their Applications, Springer, Bremen (2002).
[3] R. M. Cornell, U. Schertmann, The Iron Oxides: Structure, Properties, Reactions, Occurrence and Uses, VCH Publishers, Weinheim (2003).
[4] B. M. Berkovsky, V. F. Medvedev, M. S. Krakov, Magnetic Fluids: Engineering Applications, Oxford University Press, New York (1993).
[5] Q. A. Pankhurst, J. Connolly, S.K. Jones, J. Dobson, J. Phys. D, **36,** R167 (2003).
[6] R. Pecora, Dynamic Light Scattering, Plenum Press, New York (1985).
[7] D. Bica, L. Vékás, M. V. Avdeev, O. Marinică, V. Socoliuc, M. Bălăsoiu and V.M. Garamus, J. Magn. Magn. Mater., **311**(1), 17, (2007).
[8] L. Shen, A. Stachowiak, S.E.K. Fateen, P. E. Laibinis T. A. Hatton, Langmuir, **17**(2), 288, (2001).
[9] J.C. Bacri and R.Perzynski, Complex Fluids **415**, 99 (1993).
[10] P. J. Camp and G. N. Patey, Phys. Rev. E, **62**(4)**,** 5403 (2000).
[11] J.W. Goodman, Laser speckle and related phenomena, Vol.9 in series Topics in Applied Physics, J.C. Dainty, Ed., Springer-Verlag, Berlin, Heidelberg, New York, Tokyo, (1984).
[12] J. David Briers, Physiol. Meas. **22**, R35 (2001).
[13] D. A. Boas, A. G. Yodh, J. Opt. Soc. Am. A **14**, 192-215 (1997).
[14] Y. Aizu, T. Asakura, Opt. Las. Tech. **23**, 205 (1991).
[15] I. V. Fedosov, V. V. Tuchin, Proc. of SPIE **4434**, 192 (2001).
[16] J. D. Briers, G. Richards, X. W. He, J. Biomed. Opt. **4**, 164 (1999).
[17] D. A. Zimnyakov, J. D. Briers, V. V. Tuchin, Chap.18 in Handbook of biomedical diagnostics, Valery V. Tuchin, Ed. SPIE press, Bellingham (2002).
[18] P. Lehmann, Appl. Opt. **38**, 1144 (1999).
[19] G. Da Costa and J. Ferrari, Appl. Opt. **36**, 5231 (1997).
[20] R. Berlasso, F. Perez Quintian, M.A. Rebollo, C.A. Raffo and N.G. Gaggioli, Appl. Opt. **39**, 5811 (2000).
[21] A. Sadhwani, K.T. Schomaker, G. J. Tearney N. S. Nishioka, Appl. Opt. **35**, 5727 (1996).
[22] M. Giglio, M. Carpineti, A. Vailati and D. Brogioli, Appl. Opt. **40**, 4036-4040 (2001).
[23] Y. Piederrière, J. Cariou, Y. Guern, B. Le Jeune, G. Le Brun, J. Lotrian,, Optics Express, **12**(1), 176 (2004).
[24] Y. Piederriere, J. Le Meur, J. Cariou, J.F. Abgrall, M.T. Blouch, Optics Express **12**(19), 4596 (2004).
[25] P. Enzel, N. B. Adelman, K. J. Beckman, D. J. Campbell, A. B. Ellis, G. C. Lisensky, J. Chem.Educ., **76**, 943 (1999).
[26] R. Nothdurft, G. Yao, Optics Express **13**(25), 10034 (2005).
[27] W. Steenbergen, R.Kolkman, F. De Mul, J.Opt. Soc. Am. A, **16**, 2959 (1999)
[28] R. Bracewell, The Fourier Transform and Its Applications, 3rd ed. New York: McGraw-Hill, pp. 40-45, (1999).
[29] D. Chicea, Romanian Journal of Physics **52**(5-6), 589 (2007).
[30] D. Chicea, European Physical Journal Applied Physics **40**, 305 (2007).
[31] D. Chicea, M. Răcuciu, J. Optoelectron. Adv. Mater. **9**(12), 3843 (2007).
[32] C.F. Bohren, D. Huffman, Absorption and scattering of light by small particles, John Wiley, New York (1983).
[33] C. N. Marin, I. Mălăescu, V. Socoliuc, J. Optoelectron. Adv. Mater. **5**(1), 227 (2003).
[34] W. Tscharnuter, Photon Correlation Spectroscopy in Particle Sizing , in Encyclopedia of Analytical Chemistry, R.A. Meyers (ed), 5469, John Wiley & Sons Ltd, Chichester (2000).
[35] http://www.malvern.co.uk

*Corresponding author: dan.chicea@ulbsibiu.ro